Comparative Studies of Oxidation Processes on Group 10 Metals Dithiolene Derivatives in the Formation of Coordination Polymers

Oscar Castillo,[§] Esther Delgado,[,†] Carlos J. Gómez-García,[‡] Diego Hernández,[†] Elisa Hernández,[†] Pilar Herrasti,[#] Avelino Martín,[§] and Félix Zamora[*,†,□]*

[§]Departamento de Química Inorgánica, Universidad del País Vasco. Apartado 644, e–48080 Bilbao, Spain. [†]Departamento de Química Inorgánica, Universidad Autónoma de Madrid, 28049 Madrid, Spain. [‡]Instituto de Ciencia Molecular. Departamento de Química Inorgánica. Universidad de Valencia. C/ Catedrático José Beltrán, 2. 46980 Paterna, Valencia, Spain. [#]Departamento de Química Física Aplicada, Universidad Autónoma de Madrid, 28049 Madrid, Spain. [§]Departamento de Química Inorgánica, Universidad de Alcalá. Campus Universitario, E-28871, Alcalá de Henares, Spain. [□]Instituto Madrileño de Estudios Avanzados en Nanociencia (IMDEA Nanociencia), Cantoblanco, 28049 Madrid, Spain.

KEYWORDS: Coordination Polymers; Group 10 Metal Dithiolene Compounds; Group 10 Metal Dithiolene Ion-Pairs; Dianionic Tetranickel Dithiolene Cluster.

ABSTRACT. Air oxidation of the dithiolene derivatives $\{[K_2(\mu\text{-}H_2O)_2(\mu\text{-}thf)(thf)_2][Ni(SC_6H_2Cl_2S)_2]\}_n$ and $\{[K_2(\mu\text{-}H_2O)_2(thf)_6][Pt(SC_6H_2Cl_2S)_2]\}_n$ yielded the ion-pair compounds $[K(thf)_6][M(SC_6H_2Cl_2S)_2]$ [M = Ni or Pt] while no reaction is observed for the case of $\{[K_2(\mu\text{-}H_2O)_2(\mu\text{-}thf)(thf)_2][Pd(SC_6H_2Cl_2S)_2]\}_n$. Cyclic voltammetric studies have been used to rationalize this different behavior. Additionally, the new coordination polymers $\{[K_2(thf)_8][Ni_4(SC_6H_4S)_6]\}_n$, $\{[K_4(thf)_4(H_2O)_{2.28}][Pd(O_2SC_6H_4S)_{1.36}(OSC_6H_4S)_{0.64}]_2\}_n$, $\{[K_2(H_2O)_4][Pd(O_2SC_6H_4S)_2][Pd(O_2SC_6H_4S)(SC_6H_4S)]\}_n$ and $\{[K_4(thf)_4(H_2O)_{2.24}][Pt(O_2SC_6H_4S)_{1.38}(OSC_6H_4S)_{0.62}]_2\}_n$ have been obtained using a similar synthetic strategy *i.e.* oxidation reactions of group 10 metals dithiolene derivatives bearing $(SC_6H_4S)^{2-}$ ligands.

Introduction

Transition metal dithiolene derivatives are important research matter due to their structural diversity, redox behavior and the interesting physical properties they may exhibit.[1-15] Interestingly, dithiolene-type ligands are known as “non-innocent” because they can form complexes in different oxidation states. In fact, formation of neutral, monoanionic and dianionic dithiolene complexes is well-known.[16-19] It is noteworthy, that the oxidation processes may take place either on the metal or the dithiolene ligands, being sometimes difficult to determinate which one has been oxidized. Additionally the oxygen can also bonds to the sulfur atoms of the dithiolene ligands to form sulfinate [M-S(O)$_2$R], sulfonate [M-S(O)R] or sulfonate [M-OS(O)$_2$R] groups.[20-22]

We have recently reported the syntheses of two series of coordination polymers $\{[K_2(\mu\text{-}H_2O)_2(\mu\text{-thf})(thf)_2][M(SC_6H_2Cl_2S)_2]\}_n$ (M = Ni, Pd), $\{[K_2(\mu\text{-}H_2O)_2(thf)_6][Pt(SC_6H_2Cl_2S)_2]\}_n$, $\{[K_2(\mu\text{-}H_2O)(\mu\text{-thf})_2][Pt(SC_6H_2Cl_2S)_2]\}_n$[23] as well as $\{[K_2(\mu\text{-}H_2O)_2][Ni(SC_6H_4S)_2]\}_n$, $\{[K_2(\mu\text{-}H_2O)_2(thf)]_2[K_2(\mu\text{-}H_2O)_2(thf)_2][Pd_3(SC_6H_4S)_6]\}_n$ and $\{[K_2(\mu\text{-thf})_2][Pt(SC_6H_4S)_2]\}_n$[24] obtained by reaction of $NiCl_2{\cdot}6H_2O$, $Pd(OAc)_2$ or K_2PtCl_4 with the dithiolene $HSC_6H_2R_2SH$ (R= Cl or H) using KOH as deprotonating agent, under argon atmosphere. Following these studies, we have now carried out analogous reactions to those before described but using aerobic conditions, with the aim to prepare coordination polymers containing different d^{10} metal dithiolene derivatives as building blocks, because of the oxidation either on the metal center or the dithiolene ligand, as consequence of the metal nature or the presence/absence of donor substituent in the aromatic ring of the dithiolene used. Following this new approach we have synthesized and characterized up to six new dithiolene derivatives: the ion pair compounds $[K(thf)_6][M(SC_6H_2Cl_2S)_2]$ [M = Ni (**1**) or Pt (**2**)] and the coordination polymers $\{[K_2(thf)_8][Ni_4(SC_6H_4S)_6]\}_n$ (**3**), $\{[K_4(thf)_4(H_2O)_{2.28}][Pd(O_2SC_6H_4S)_{1.36}(OSC_6H_4S)_{0.64}]_2\}_n$ (**4**), $\{[K_2(H_2O)_4][Pd(O_2SC_6H_4S)_2][Pd(O_2SC_6H_4S)(SC_6H_4S)]\}_n$ (**5**) and $\{[K_4(thf)_4(H_2O)_{2.24}][Pt(O_2SC_6H_4S)_{1.38}(OSC_6H_4S)_{0.62}]_2\}_n$ (**6**).

Experimental Section

All the reagents and solvents are commercial available and were used as received without further purification. Elemental analyses were performed on a LECO CHNS-932 Analyzer.

Cyclic voltammetry experiments were recorder using an AUTOLAB 30. The experiments were performed in a conventional three electrode cell, with a glassy carbon and platinum electrodes used as working and counter-electrode, respectively. All the potentials in this work are stated against the Ag/AgCl electrode (3 M KCl). The supporting electrolyte was a 0.1 M solution of tetra-*n*-butylammonium hexafluorophosphate dissolved in methanol. The experiments were performed under nitrogen atmosphere and a scan rate of 100 mV s^{-1}.

Crystal structure determination of complexes 1-6. Single crystals of compounds **1**-**6** were covered with a layer of a viscous perfluoropolyether (Fomblin®Y), mounted on a cryoloop™ (**1**-**3** and **5**) or Micromount™ (**4** and **6**) with the aid of a microscope and immediately placed in the low temperature nitrogen stream of the diffractometer. The intensity data sets were collected at 200 K on a Bruker-Nonius KappaCCD (**1**-**3**, **5**) or Bruker Kappa Apex II (**4**, **6**) diffractometer equipped with an Oxford Cryostream 700 unit. The structures were solved, by using the WINGX package[25] by direct methods (SHELXS-2013[26,27] for complexes **1-3** and **5**) (SHELXS-97[26] for **4** and **6**) and refined by least-squares against F^2 (SHELXL-2014[27]). All the hydrogen atoms were positioned geometrically and refined by using a riding model, except those belonging to the water molecules of compound **5** whose coordinates were constrained by DFIX commands but using thermal isotropic displacement parameters related to that of the parent oxygen atom. All the non-hydrogen atoms were refined anisotropically.

Compounds **4** and **6** showed a more complex disorder due to the presence of a non-ordered mixture of the 2-sulfanylbenzenesulfinate (68 % and 69 %, respectively) and 2-sulfanylbenzenesulfenate (32 % and 31 %, respectively) molecules chelating the metal center. This occupational disorder also generates a positional one of the potassium cations that interacts with these molecules and of the water molecules that complete the coordination sphere.

Refinement convergence could only be reached after applying EADP restraint to all the disordered atoms.

The highest peak of 2.718 eÅ^{-3} in the study of **4** was found at 0.10 Å from Pd1, but other peaks with slightly lower electronic density could not be assigned to disordered carbon atoms or removed by using the squeeze procedure, which led to a poor-quality refinement.

Crystals of compound **5** crystallized with an unknown number of solvent molecules, and it was not possible to get sensible chemical models for them. The Squeeze procedure of the PLATON package[28] was employed to remove the contribution of that electronic density to the structure factors, obtaining a solvent accessible volume of 14.2 % of the unit cell volume. Crystallographic data for compounds **1**–**6** are summarized in Table 1 (CCDC 1582337, 1582338 and 1583016-1583019).

Magnetic susceptibility measurements were performed with a Quantum Design MPMS-XL-5 SQUID magnetometer in the temperature range 2-300 K with a magnetic field of 0.5 T on polycrystalline samples of compounds **1**-**4** immersed in their mother liquor (with dry masses of 27.46, 29.57, 10.31 and 8.79 mg, respectively). Susceptibility data were corrected for the sample holder and solvent and for the diamagnetic contribution of the salts using Pascal's constants.[29]

The DC electrical conductivity was measured in the temperature range 100-400 K with the two or four contacts method (depending on the size of the crystals) on several single crystals of compounds **1**-**4**. Crystals of compounds **1**-**4** were measured in three or four consecutive scans: they were initially cooled from 300 to 100-200 K (since at lower temperatures the resistance was above the detection limit of our equipment, 5×10^{11} Ω), then heated from 200 to 400 K and then cooled again from 400 to 200 or to 300 K.

The contacts were made with Pt wires (25 μm diameter) using graphite paste. The samples were measured in a Quantum Design PPMS-9 equipment connected to an external voltage source (Keithley model 2450 source-meter) and amperometer (Keithley model 6514 electrometer). Since the crystals loose crystallinity very fast, they were covered with paraffin oil immediately after the contacts where done. All the conductivity quoted values have been measured in the voltage range where the crystals are Ohmic conductors. The cooling and warming rates were 1 and 2 K min^{-1}.

Syntheses of compounds $[K(thf)_6][M(SC_6H_2Cl_2S)_2]$ [M = Ni (1), Pt (2)]. A mixture of 1,2-$HSC_6H_2Cl_2SH$ (266 mg, 1.27 mmol) and 10 mL of an 5 % aqueous solution of KOH was stirred for 5 min. Then, a solution of $NiCl_2 \cdot 6H_2O$ (150 mg, 0.63 mmol) in 10 mL of EtOH/H_2O (1:1) was slowly added and the mixture stirred at 20 ºC for 30 min and the solvent was removed until dryness. The solid residue was washed with *n*-hexane and the residue extracted in THF. A flow of air was bubbled into the red THF solution for 1 h. Finally, the solvent was removed and the residue crystallized in wet THF/*n*-heptane (1:1) at -20 ºC, yielding suitable crystals for X-ray analysis of $[K(thf)_6][Ni(SC_6H_2Cl_2S)_2]$ (**1**) (370 mg; 61.9 %). Similar reaction but using K_2PtCl_4 (150 mg, 0.36 mmol) as starting material and after keeping the mixture stirring for 3.5 h, yielded compound $[K(thf)_6][Pt(SC_6H_2Cl_2S)_2]$ (**2**) (265 mg; 67.8 %). Anal. Calcd. (Found) for $C_{28}H_{36}Cl_4KNiO_4S_4$ (**1**-2THF): C, 41.81 (39.89); H, 4.51 (4.33); S, 15.94 (15.55) %. Anal. Calcd. (Found) for $C_{32}H_{44}Cl_4KO_5PtS_4$ (**2**-THF): C, 37.94 (37.81); H, 4.38 (4.54); S, 12.66 (11.09) %.

Synthesis of compound $\{[K_2(thf)_8][Ni_4(SC_6H_4S)_6]\}_n$ (3). A solution of $NiCl_2 \cdot 6H_2O$ (150 mg, 0.63 mmol) in 10 mL of EtOH/H_2O (1:1) was slowly added to a mixture of HSC_6H_4SH (181 mg, 1.27 mmol) in 10 mL of a 5 % aqueous solution of KOH. The reaction was stirred at 20 ºC for 30 minutes and the solvent was removed in vacuum until dryness and the residue extracted in THF.

Then a flow of air was bubbled into this solution for 1 hour. Finally, the solvent was removed to dryness and the residue crystallized in wet THF/*n*-heptane (1:1) to yield compound **3** (70 mg, 43.71 %). Anal. Calcd. (Found) for $C_{52}H_{56}K_2Ni_4O_4S_{12}$ (**3**-4THF): 43.29 (41.58); 3.91 (3.80); 26.67 (23.63) %.

Syntheses of compounds $\{[K_4(thf)_4(H_2O)_{2.28}][Pd(O_2SC_6H_4S)_{1.36}(OSC_6H_4S)_{0.64}]_2\}_n$ (4) and **$\{[K_2(H_2O)_4][Pd(O_2SC_6H_4S)_2][Pd(O_2SC_6H_4S)(SC_6H_4S)]\}_n$ (5).** Following the same procedure described for compound **3** but using $Pd(OAc)_2$ and 2 days of stirring instead, a change in the solution color from red to red-brown was observed. Then, the solvent was removed and the residue crystallized in wet THF/*n*-heptane (1/1) to yield crystals of compound $\{[K_4(thf)_4(H_2O)_{2.28}][Pd(O_2SC_6H_4S)_{1.36}(OSC_6H_4S)_{0.64}]_2\}_n$ (**4**) (45 mg, 27.2 %) together with a few crystals of compound $\{[K_2(H_2O)_4][Pd(O_2SC_6H_4S)_2][Pd(O_2SC_6H_4S)(SC_6H_4S)]\}_n$ (**5**). Anal. Calcd. (Found) for $C_{36}H_{40}K_4O_{12}Pd_2S_8$ (**4**-THF): C, 33.51 (33.95); H, 3.12 (3.58); S, 19.88 (17.04) %.

Synthesis of compound $\{[K_4(thf)_4(H_2O)_{2.24}][Pt(O_2SC_6H_4S)_{1.38}(OSC_6H_4S)_{0.62}]_2\}_n$ (6). Following the same procedure used for compound **3** but using K_2PtCl_4 as starting material, a few crystals of compound $\{[K_4(thf)_4(H_2O)_{2.24}][Pt(O_2SC_6H_4S)_{1.38}(OSC_6H_4S)_{0.62}]_2\}_n$ (**6**) were obtained upon crystallization in THF/*n*-heptane (1:1) at room temperature.

Results and Discussion

The observed change in the color of the solution of compounds $\{[K_2(\mu\text{-}H_2O)_2(\mu\text{-}thf)(thf)_2][Ni(SC_6H_2Cl_2S)_2]\}_n$ and $\{[K_2(\mu\text{-}H_2O)_2(thf)_6][Pt(SC_6H_2Cl_2S)_2]\}_n$, from red to green, when they were stored in air, prompted us to study in detail their behavior under aerobic

conditions. Thus, after carrying out the reactions described to prepare compounds $\{[K_2(\mu\text{-}H_2O)_2(\mu\text{-thf})(thf)_2][Ni(SC_6H_2Cl_2S)_2]\}_n$ and $\{[K_2(\mu\text{-}H_2O)_2(thf)_6][Pt(SC_6H_2Cl_2S)_2]\}_n$,[23] air was bubbled during one hour into their THF solutions in order to oxidize them (see Experimental Section). Then, the solvent was removed to dryness and the residue crystallized in THF/*n*-heptane yielding crystals of compounds $[K(thf)_6][M(SC_6H_2Cl_2S)_2]$ [M = Ni (**1**), Pt (**2**)] suitable for X-ray analysis (Scheme 1). Contrarily, any modification was observed in the solution color of the palladium compound $\{[K_2(\mu\text{-}H_2O)_2(\mu\text{-thf})(thf)_2][Pd(SC_6H_2Cl_2S)_2]\}_n$ after bubbling air and also, all attempts to grow suitable crystals for X-ray diffraction failed.

The compounds $[K(thf)_6][M(SC_6H_2Cl_2S)_2]$ [M = Ni (**1**), Pt (**2**)] are isostructural and consist of anion-cation pairs (Figures 1 and S1). The cationic entities are formed by octahedral potassium complexes in which the metal center is coordinated to six oxygen atoms of six different THF ligands, while the anionic moieties are based on a centrosymmetric square planar nickel or platinum complex formed by coordination of the metal center to four sulfur atoms of two dithiolene ligands. The main difference between both crystal structures comes from the significantly longer M-S bond distances for the platinum compound (2.144-2.148 Å in **1** *vs.* 2.262-2.264 Å in **2**). These anionic complexes are held together by means of weak S···H-C interactions [d(S-C) = 3.689 Å for **1**, and 3.641 Å for **2**], generating supramolecular herringbone shaped sheets in the (10-1) plane (Figure 1). The cationic entities are located between the anionic supramolecular sheets just above and below the voids within the herringbone supramolecular sheet.

In order to rationalize the different behavior of the palladium derivative to the oxidation process, as compare with the nickel and platinum ones, we carried out cyclic voltammetry studies on the precursors.[23]

As it shows in Figure 2, two different oxidation processes ascribed to the $2^-/1^-$ and $1^-/0$ couples respectively, are observed for the compounds $\{[K_2(\mu\text{-}H_2O)_2(\mu\text{-}thf)(thf)_2][Ni(SC_6H_2Cl_2S)_2]\}_n$ (-0.142 and 0.540 V), $\{[K_2(\mu\text{-}H_2O)_2(\mu\text{-}thf)(thf)_2][Pd(SC_6H_2Cl_2S)_2]\}_n$ (0.117 and 0.527 V) and $\{[K_2(\mu\text{-}H_2O)_2(thf)_6][Pt(SC_6H_2Cl_2S)_2]\}_n$ (-0.125 and 0.550 V). The fact that a positive value is found for the first oxidation process in the Pd derivative as compare with those negative potentials exhibit by the related Ni and Pt highlights the difficulty to obtain the corresponding palladium oxidized complex. The first oxidation process is quasi-reversible for the three complexes, being the second one irreversible in all cases. Some theoretical and experimental studies on the redox processes of group 10 metals dithiolene derivatives have been reported confirming the lesser tendency of the oxidation of $[ML_2]^{2-}$ to $[ML_2]^-$ for the palladium compounds.[30,31]

In order to complete the study on the oxidation processes of group 10 metal dithiolene derivatives, we have carried out similar reactions bubbling a flow of air into THF solutions containing $\{[K_2(\mu\text{-}H_2O)_2][Ni(SC_6H_4S)_2]\}_n$, $\{[K_2(\mu\text{-}H_2O)_2(thf)]_2[K_2(\mu\text{-}H_2O)_2(thf)_2][Pd_3(SC_6H_4S)_6]\}_n$ and $\{[K_2(\mu\text{-}thf)_2][Pt(SC_6H_4S)_2]\}_n$ with the aim to obtain the corresponding oxidized species (Scheme 1). These reactions have allowed us to isolate and to characterize four new derivatives in which the oxidation takes place either on the metal center, as in compound **3**, or on the sulfur atoms of the dithiolene ligand, to produce a mixture of 2-sulfanylbenzenesulfinate and 2-sulfanylbenzenesulfenate, as observed in compounds **4** and **6**, or a mixture of 2-sulfanylbenzenesulfinate and 1,2-benzenedithiolene for compound **5**.

The crystal structure of compound **3** consists of linear tetranuclear $[Ni_4(SC_6H_4S)_6]^{2-}$ entities in which two crystallographically independent metal centers can be distinguished, Ni1 located in the two central positions and Ni2 located in the edges of the tetramer (Figure 3). The metal Ni2

atoms adopt a square planar coordination geometry which is quite common for Ni(II) metal centers (d^8), but Ni1 atoms are located inside a nearly square pyramid coordination environment so they have been assumed to correspond to Ni(III) metal centers. All the 1,2-benzenedithiolene ligands adopt the same μ-κS,S′:κS coordination mode towards the nickel atoms imposing Ni1···Ni1 and Ni1···Ni2 distances of 3.126 and 2.901 Å, respectively. The four 1,2-benzedithiolene ligands placed at the edges of the tetrameric entity are also involved in the coordination of the charge balancing potassium cations. In fact, the potassium atoms are coordinated to four THF molecules and three sulfur atoms from two nickel-dithiolene entities. This coordination bond network gives rise to a 1D coordination polymer in which the tetrameric $[Ni_4(SC_6H_4S)_6]^{2-}$ entities are bridged by double $[K(thf)_4]^+$ entities that share two sulfur donor atoms of their octahedral coordination sphere. The benzene rings and the THF molecules are located on the external surface of these chains that are held together by weak van der Waals interactions without any evidence of aromatic ones.

Although the ion pair $[K(15\text{-crown-}5)_2]_2[Ni_4(\alpha\text{-tpdt})_6]$ containing a dianionic Ni_4 cluster moiety had been reported,[32] as far as we know, compound **3** is the first example where these dianionic entities are connected through alkali complexes yielding the coordination polymer $\{[K_2(thf)_8][Ni_4(SC_6H_4S)_6]\}_n$.

As previously stated, compound **4** contains a mixture of 2-sulfanylbenzenesulfinate (70 %) and 2-sulfanylbenzenesulfenate (30 %) as randomly distributed palladium chelating ligands. The 2-sulfanylbenzenesulfenate anion can be considered as an intermediate of the oxidation of 1,2-benzenedithiolene into 2-sulfanylbenzenesulfinate. Despite the partial oxidation of the dithiolene ligand, the *in situ* generated new ligands retain the κS, κS′ chelation mode. The palladium metal center shows a square planar coordination geometry formed by four sulfur atoms, with the

sulfinate/sulfenate groups arranged in cis conformation (Figure 4). The dihedral angle between the two-coordinated benzene aromatic rings is 163.4º. The charge balancing potassium cations now complete their coordination sphere not only with the thiolate sulfur atoms, THF and water molecules but also with the oxygen atoms of the sulfinate and sulfenate groups. However, the random alternation of these ligands implies the presence of a disorder on the position of one of the potassium cations (the one interacting with the second oxygen atom of the sulfinate group which is not present in the sulfenate group) and on the water molecules that complete its coordination sphere.

In order to provide a clearer description of the crystal structure, we just focus on the sulfinate counterpart that represents the main contribution to the disorder. There are two crystallographically independent potassium metal centers: K1, which is coordinated to four thiolate sulfur atoms, two oxygen from two sulfinate groups and a water molecule, and K2, which is coordinated to six oxygen atoms from four sulfinate groups and two THF molecules. The resulting coordination bond network corresponds to a 2D coordination polymer. The benzene rings and THF molecules are decorating the external surface of the sheets.

Compound **5** contains two different square planar palladium entities: $[Pd(O_2SC_6H_4S)_2]^{2-}$ and $[Pd(SC_6H_4S)(O_2SC_6H_4S)]^{2-}$ (Figure 5). In contrast to compound **4**, these two entities are well ordered along the crystal structure. As a consequence, the charge balancing potassium cations that interact with these entities are also ordered. The palladium entities present the previously described roof shape with the benzene rings forming dihedral angles of 158.2 and 161.5º between them. Although all the potassium cations are heptacoordinated, two different coordination environments can be distinguished: K1 is surrounded by two oxygen atoms from the sulfinate groups, three thiolate sulfur atoms, and two water molecules, whereas K2 is

coordinated to four thiolate sulfur atoms, one oxygen from a sulfinate group and two water molecules. This scheme of coordination bonds generates a 1D coordination polymer that exposes not only the benzene rings but also the coordinating water molecules as hydrogen bond donors and some uncoordinated sulfinate oxygen atoms as acceptors. Consequently, the packing of these chains is dictated by the geometrical restraints imposed by the highly directional hydrogen bonding interactions with the help of some T-shaped aromatic interactions. This quite rigid packing leaves some voids that are occupied by solvent molecules (14.2 % of the volume).

Compound **6** (Figure S2) is isostructural to compound **4** just replacing the palladium metal centers by platinum ones. It also presents the same occupational disorder between the 2-sulfanylbenzenesulfinate (69 %) and 2-sulfanylbenzenesulfenate (31 %) ligands that induces a positional disorder in one of the charge balancing potassium cations.

It is worth mentioning that despite this fact, 2-sulfanylbenzenesulfinate and 2-sulfanylbenzenesulfenate ligands present a similar chelating mode involving the sulfur atoms giving rise to closely related quasi planar $[M^{II}(SC_6H_4S\text{-}\kappa S,S'$ or $O_2SC_6H_4S\text{-}\kappa S,S')_2]^{2-}$ (M^{II} = Ni, Pd, Pt) entities with the exception of compound **3**. The last compound presents some singularities as the presence of both Ni(II) and Ni(III) metal centers within a linear tetrameric entity of formula $[Ni_4(\mu\text{-}SC_6H_4S\text{-}\kappa S,S':\kappa S)_6]^{2-}$. In all cases the anionic charge of the transition metal complex entities is balanced by the presence of potassium counterions that are coordinated to the sulfur donor atoms of the dithiolene and sulfinate/sulfenate ligands but also to a variable amount of solvent molecules.

Physical Properties

Magnetic Properties. Magnetic susceptibility measurements carried out on the crystals immersed in their mother liquor to avoid loss of coordinating solvent for compounds **1**-**4** show that compounds **1** and **2** have one unpaired electron per metal atom, whereas compound **3** has two Ni(III) and two Ni(II) ions per Ni_4 tetramer, in agreement with the structural data. Finally, compound **4** is diamagnetic, in agreement with the structural data. Thus, the $\chi_m T$ product (χ_m is the molar magnetic susceptibility per formula unit) for compounds **1** and **2** shows a value close to 0.4 cm^3 K mol^{-1} at high temperatures, close to the expected value for one unpaired electron with g = 2 (Figure 6). When the samples are cooled, $\chi_m T$ remains constant down to *ca*. 50 K and shows a progressive decrease at lower temperatures to reach values of *ca*. 0.04 and 0.11 cm^3 K mol^{-1} for **1** and **2**, respectively (Figure 6). This behavior suggests the presence of moderate antiferromagnetic interactions in both compounds. Among the several models that can be used to fit the magnetic properties, we have tried a S =1/2 dimer,[33] a regular S= 1/2 antiferromagnetic chain[34] and a quadratic S = ½ layer antiferromagnetic (QLAF)[35] models, all of them with a paramagnetic monomeric contribution. Although the two last models give satisfactory fits, we have chosen the 2D QLAF one since the structure of compounds **1** and **2** shows that the intermolecular C-H···S interactions give rise to a 2D structure (Figure 1). This 2D QLAF model reproduces very satisfactorily the magnetic properties of these compounds with the following parameters: g = 2.074, J = -6.4 cm^{-1} and a paramagnetic S = ½ impurity, c = 1.4 % for **1** and g = 2.022, J = -6.6 cm^{-1} and c = 2.0 % for **2** (solid lines in Figure 6, the Hamiltonian is written as $H = -J S_i S_{i+1}$).

Compound **3** shows a similar behavior to **1** and **2** but now the $\chi_m T$ value per Ni_4 tetramer is *ca*. 0.75 cm^3 K mol^{-1}, which is the expected value for two non-interaction electrons. When cooling the sample, $\chi_m T$ remains constant down to *ca*. 100 K and below this temperature it shows a

progressive decrease to reach a value of *ca*. 0.44 cm^3 K mol^{-1} at 2 K (Figure 6). The $\chi_m T$ value at room temperature suggests that there are two S = ½ contributions per Ni tetramer, in agreement with the structural data that suggests the presence of two Ni(III) ions in the central part of the tetramer. Since these two Ni(III) ions are connected through a double sulfur bridge, we have fit the magnetic properties of compound **3** with a simple S = ½ dimer model. Since, this model is not able to reproduce the magnetic properties in a satisfactory way, we have included an inter-dimer interaction (zj) with the molecular field approximation.[36,37] This model reproduces very satisfactorily the magnetic properties of compound **3** with the following parameters: g = 2.037, J = -28.1 cm^{-1}, zj = -7.0 cm^{-1} and c = 9.9 % (solid line in Figure 6, the Hamiltonian is written as $H = -J S_1S_2$).

Finally, compound **4** shows an almost zero signal (Figure 6), indicating that it is essentially diamagnetic, in agreement with the presence of a d^8 square planar Pd(II) ion, as observed in its structure.

The presence of one unpaired electron per metal center in compounds **1** and **2**, as shown by the magnetic measurements, confirms the oxidation of both compounds. On the other hand, the presence of weak antiferromagnetic couplings in both compounds indicates that the paramagnetic spin density is also partially delocalized over the dithiolene ligand. A close look at the structure of **1** and **2** shows the presence of intermolecular C-H···S interactions implying the S atoms of the dithiolene ligands and the external C atoms of a contiguous $M(SC_6H_2Cl_2S)_2$ unit (with a shortest S···C distance of 3.689(8) Å). This interaction leads to a bidimensional supramolecular network from the structural point of view (Figure 1), in agreement with the magnetic results.

In compound **3** the observed $\chi_m T$ value confirms the presence of two diamagnetic d^8 square planar Ni(II) ions and two paramagnetic d^7 Ni(III) ions. As in **1** and **2**, the presence of weak interdimer interactions indicates the partial delocalization of the unpaired spin density over the dithiolene ligands.

Electrical Properties. Compounds **1**-**4** are semiconductors with room temperature conductivities in the range 10^{-5}-10^{-8} S/cm (Table 2).

All the crystals where initially cooled from 300 to 100-200 K until the resistance of the sample reached the detection limit of our equipment (5×10^{11} Ω) (Figure 7). This initial cooling scan shows a fast increase of the resistivity as the temperature is lowered with very high activation energies of *ca*. 2000 meV in compounds **1** and **3**. This behavior indicates an initial loss of solvent and, therefore, an irreversible partial loss of crystallinity. Once the resistance reaches saturation, the samples were heated up to 400 K. As expected, in all compounds the resistivity of the heating scan is higher than the one observed in the initial cooling scan, suggesting a progressive irreversible degradation of the sample when it is submitted to low pressure (probably due to a loss of crystallinity as a result of some solvent lost). During the first heating scan all the samples show semiconducting behaviors with activation energies in the range 200-1100 meV (Table 2). Samples **2**-**4** show resistivity minima at *ca*. 310-350 K (Figure 7). On further heating, these samples show resistivity increases reaching maxima at *ca.* 360-380 K to decrease again until 400 K. This behavior suggests that samples **2**-**4** suffer a thermal degradation at high temperatures responsible of the increase in the resistivity. When crystals of compounds **2**-**4** are cooled from 400 K to 200-300 K they all show much higher resistivity values and higher activation energies (in the range 800-1400 meV, Table 2, Figure S3 than those observed during

the heating scan, indicating that the thermal degradation during the first heating scan is irreversible. Compound **1** shows a higher thermal stability and, even after three cooling/heating scans, the crystals retain their initial behavior (Figure 7).

In all cases the relatively similar electrical conductivities and activation energies can be attributed to the presence of similar pathways for the electron delocalization implying the M-dithiolene units, the S···H-C, Cl···Cl and K-O interactions. The complexity of the possible delocalization pathways and the presence of solvent molecules that are easily lost precludes any correlation between the structure and the electrical conductivity. Nevertheless, the similarity of the conductivity values observed in the four samples suggests that the mechanism must be similar and imply the short S···C contacts observed between different dithiolene units.

Conclusions

In summary, different type of compounds have been obtained from the reactions of group 10 metal reagents with $HSC_6H_2X_2SH$ (X= Cl or H) under aerobic conditions, depending on the metal and the dithiolene. Thus, isostructural Ni and Pt ion-pair derivatives have been isolated in the case of the substituted dithiolene $HSC_6H_2Cl_2SH$, while coordination polymers are formed for all metals when HSC_6H_4SH is used instead. Among these polymers, it is remarkable the formation of compound $\{[K_2(thf)_8][Ni_4(SC_6H_4S)_6]\}_n$ being the first example of a coordinating polymer containing a mixture balance tetranuclear cluster as negative entity.

Supporting Information. A pdf file with additional information on physical properties is available free of charge. Files in CIF format for compounds **1-6** are (CCDC refs.: 1582337, 1582338 and 1583016-1583019) available free of charge.

ACKNOWLEDGMENT

This work was supported in part by MICINN (grants MAT2016-77608-C3-1-P, MAT2016-75883-C2-1-P, CTQ2013-44625-R and and CTQ2017-87201-P) and Generalitat Valenciana (PrometeoII/2014/076).

References

1. Robertson, N.; Cronin, L. Metal bis-1,2-dithiolene complexes in conducting or magnetic crystalline assemblies. *Coord. Chem. Rev.* **2002**, *227*, 93-127.

2. *Dithiolene Chemistry: Synthesis, Properties and applications;* Progress in Inorganic Chemistry; John Wiley & Sons, Inc.: New York, 2004; Vol. 52.

3. Muller-Westerhoff, U. T.; Vance, B. *Comprehensive coordination chemistry;* Pergamon Press: Oxford, U. K., 1987; Vol. 2.

4. Clemenson, P. I. The Chemistry and Solid State Properties of Nickel, Palladium and Platinum Bis(Maleonitriledithiolate) Compounds. *Coord. Chem. Rev.* **1990**, *106*, 171-203.

5. Ezzaher, S.; Gogoll, A.; Bruhn, C.; Ott, S. Directing protonation in [FeFe] hydrogenase active site models by modifications in their second coordination sphere. *Chem. Commun.* **2010**, *46*, 5775-5777.

6. Alcácer, L.; Novais, H. Linear Chain 1,2-Dithiolene Complexes. In *Extended Linear Chain Compounds.*; Miller, J. S., Ed.; Springer US: New York, 1983; Vol. Cap. 6, 319-351.

7. Cassoux, P.; Valade, L.; Kobayashi, H.; Kobayashi, A.; Clark, R. A.; Underhill, A. E. Molecular metals and superconductors derived from metal complexes of 1,3-dithiol-2-thione-4,5-dithiolate (dmit). *Coord. Chem. Rev.* **1991**, *110*, 115-160.

8. Sproules, S.; Wieghardt, K. o-Dithiolene and o-aminothiolate chemistry of iron: Synthesis, structure and reactivity. *Coord. Chem. Rev.* **2010**, *254*, 1358-1382.

9. Garreau de Bonneval, B.; Moineau-Chane Ching, K. I.; Alary, F.; Bui, T. T.; Valade, L. Neutral d8 metal bis-dithiolene complexes: Synthesis, electronic properties and applications. *Coord. Chem. Rev.* **2010**, *254*, 1457-1467.

10. Alvarez, S.; Vicente, R.; Hoffmann, R. Dimerization and stacking in transition-metal bisdithiolenes and tetrathiolates. *J. Am. Chem. Soc.* **1985**, *107*, 6253-6277.

11. Takaishi, S.; Hosoda, M.; Kajiwara, T.; Miyasaka, H.; Yamashita, M.; Nakanishi, Y.; Kitagawa, Y.; Yamaguchi, K.; Kobayashi, A.; Kitagawa, H. Electroconductive Porous Coordination Polymer Cu[Cu(pdt)2] Composed of Donor and Acceptor Building Units. *Inorg. Chem.* **2009**, *48*, 9048-9050.

12. Ribas, X.; Dias, J. C.; Morgado, J.; Wusrt, K.; Santos, I. C.; Almeida, M.; Vidal-Gancedo, J.; Veciana, J.; Rovira, C. Alkaline Side-Coordination Strategy for the Design of Nickel(II) and Nickel(III) Bis(1,2-diselenolene) Complex Based Materials. *Inorg. Chem.* **2004**, *43*, 3631-3641.

13. Llusar, R.; Uriel, S.; Vicent, C.; Clemente-Juan, J.; Coronado, E.; Gómez-García, C. J.; Braïda, B.; Canadell, E. Single-Component Magnetic Conductors Based on Mo_3S_7 Trinuclear Clusters with Outer Dithiolate Ligands. *J. Am. Chem. Soc.* **2004**, *126*, 12076-12083.

14. Llusar, R.; Triguero, S.; Polo, V.; Vicent, C.; Gómez-García, C. J.; Jeannin, O.; Fourmigué, M. Trinuclear Mo_3S_7 Clusters Coordinated to Dithiolate or Diselenolate Ligands and Their Use in the Preparation of Magnetic Single Component Molecular Conductors. *Inorg. Chem.* **2008**, *47*, 9400-9409.

15. Gushchin, A. L.; Llusar, R.; Vicent, C.; Abramov, P. A.; Gómez-Garcia, C. J. Mo_3Q_7 (Q = S, Se) Clusters Containing Dithiolate/Diselenolate Ligands: Synthesis, Structures, and Their Use as Precursors of Magnetic Single-Component Molecular Conductors. *Eur. J. Inorg. Chem.* **2013**, 2615-2622.

16. Belo, D.; Almeida, M. Transition metal complexes based on thiophene-dithiolene ligands. *Coord. Chem. Rev.* **2010**, *254*, 1479-1492.

17. Lim, B. S.; Fomitchev, D. V.; Holm, R. H. Nickel Dithiolenes Revisited: Structures and Electron Distribution from Density Functional Theory for the Three-Member Electron-Transfer Series $[Ni(S_2C_2Me_2)_2]^{0,1-,2-}$. *Inorg. Chem.* **2001**, *40*, 4257-4262.

18. Eisenberg, R.; Gray, H. B. Noninnocence in Metal Complexes: A Dithiolene Dawn. *Inorg. Chem.* **2011**, *50*, 9741-9751.

19. Zarkadoulas, A.; Field, M. J.; Papatriantafyllopoulou, C.; Fize, J.; Artero, V.; Mitsopoulou, C. A. Experimental and Theoretical Insight into Electrocatalytic Hydrogen Evolution with Nickel Bis(aryldithiolene) Complexes as Catalysts. *Inorg. Chem.* **2016**, *55*, 432-444.

20. Buonomo, R. M.; Font, I.; Maguire, M. J.; Reibenspies, J. H.; Tuntulani, T.; Darensbourg, M. Y. Study of Sulfinate and Sulfenate Complexes Derived from the Oxygenation of Thiolate

Sulfur in 1,5-Bis(2-mercapto-2-methylpropyl)-1,5-diazacyclooctanato(2-)]nickel(II). *J. Am. Chem. Soc.* **1995**, *117*, 963-973.

21. Henderson, R. K.; Bouwman, E.; Spek, A. L.; Reedijk, J. A Unique Mononuclear Nickel Disulfonato Complex Obtained by Oxidation of a Mononuclear Nickel Dithiolate Complex. *Inorg. Chem.* **1997**, *36*, 4616-4617.

22. Bolligarla, R.; Das, S. K. Sulfur Oxygenation of $[Ni(btdt)_2]^{2-}$ by Aerial Oxidation under Ambient Conditions – Syntheses, Crystal Structures, and Properties of $[Bu_4N]_2[Ni(btdt)_2]$ and $[Bu_4N]_2[Ni(btdtO_2)_2]\cdot H_2O$ ($\{btdt\}^{2-}$ = 2,1,3-Benzenethiadiazole-5,6-dithiolate). *Eur. J. Inorg. Chem.* **2012**, 2933-2939.

23. Delgado, E.; Gómez-García, C. J.; Hernández, D.; Hernández, E.; Martín, A.; Zamora, F. Unprecedented layered coordination polymers of dithiolene group 10 metals: magnetic and electrical properties. *Dalton Trans.* **2016**, *45*, 6696-6701.

24. Castillo, O.; Delgado, E.; Gómez-García, C. J.; Hernández, D.; Hernández, E.; Martín, A.; Martínez, J. I.; Zamora, F. Group 10 Metal Benzene-1,2-dithiolate Derivatives in the Synthesis of Coordination Polymers Containing Potassium Countercations. *Inorg. Chem.* **2017**, *56*, 11810-11818.

25. Farrugia, L. J. WinGX and ORTEP for Windows: an update. *J. Appl. Cryst.* **2012**, *45*, 849-854.

26. Sheldrick, G. M. A short history of SHELX. *Acta Crystallogr.* **2008**, *A64*, 112-122.

27. Sheldrick, G. M. Crystal structure refinement with SHELXL. *Acta Crystallogr.* **2015**, *C71*, 3-8.

28. Spek, A. L. PLATON SQUEEZE: a tool for the calculation of the disordered solvent contribution to the calculated structure factors. *Acta Crystallogr.* **2015**, *C71*, 9-18.

29. Bain, G. A.; Berry, J. F. Diamagnetic corrections and Pascal's constants. *J. Chem. Educ.* **2008**, *85*, 532-536.

30. Saito, G.; Izukashi, H.; Shibata, M.; Yoshida, K.; Kushch, L. A.; Kondo, T.; Yamochi, H.; Drozdova, O. O.; Matsumoto, K.; Kusunoki, M.; Sakaguchi, K. I.; Kojima, N.; Yagubskii, E. B. Formation of 2 : 1 insulating complexes of $D^{+\cdot}$ $D^{+\cdot}$ A^{2-} alternating stack and a 4 : 1 semimetallic complex using M(dto)2 dianions (M = Ni, Pd or Pt and dto = dithiooxalate). *J. Mater. Chem.* **2000**, *10*, 893-910.

31. Espa, D.; Pilia, L.; Makedonas, C.; Marchiò, L.; Mercuri, M. L.; Serpe, A.; Barsella, A.; Fort, A.; Mitsopoulou, C. A.; Deplano, P. Role of the Acceptor in Tuning the Properties of Metal [M(II) = Ni, Pd, Pt] Dithiolato/Dithione (Donor/Acceptor) Second-Order Nonlinear Chromophores: Combined Experimental and Theoretical Studies. *Inorg. Chem.* **2014**, *53*, 1170-1183.

32. Neves, A. I. S.; Santos, I. C.; Pereira, L. C. J.; Rovira, C.; Ruiz, E.; Belo, D.; Almeida, M. Ni-2,3-thiophenedithiolate Anions in New Architectures: An In-Line Mixed-Valence Ni Dithiolene (Ni_4–S_{12}) Cluster. *Eur. J. Inorg. Chem.* **2011**, 4807-4815.

33. Bleaney, B.; Bowers, K. D. Anomalous paramagnetism of copper acetate. *Proc. R. Soc. Lond. A* **1952**, *214*, 451-465.

34. Estes, W. E.; Gavel, D. P.; Hatfield, W. E.; Hodgson, D. J. Magnetic and structural characterization of dibromo- and dichlorobis(thiazole)copper(II). *Inorg. Chem.* **1978**, *17*, 1415-1421.

35. Lines, M. E. The quadratic-layer antiferromagnet. *Journal of Physics and Chemistry of Solids* **1970**, *31*, 101-116.

36. O'Connor, C. J. Magnetochemistry. Advances in Theory and Experimentation. *Progress in Inorganic Chemistry*; Lippard, S. J., Ed.; John Wiley & Sons, Inc.: 1982; 203-283.

37. Kahn, O. *Molecular magnetism;* VCH-Publishers: USA, 1993 .

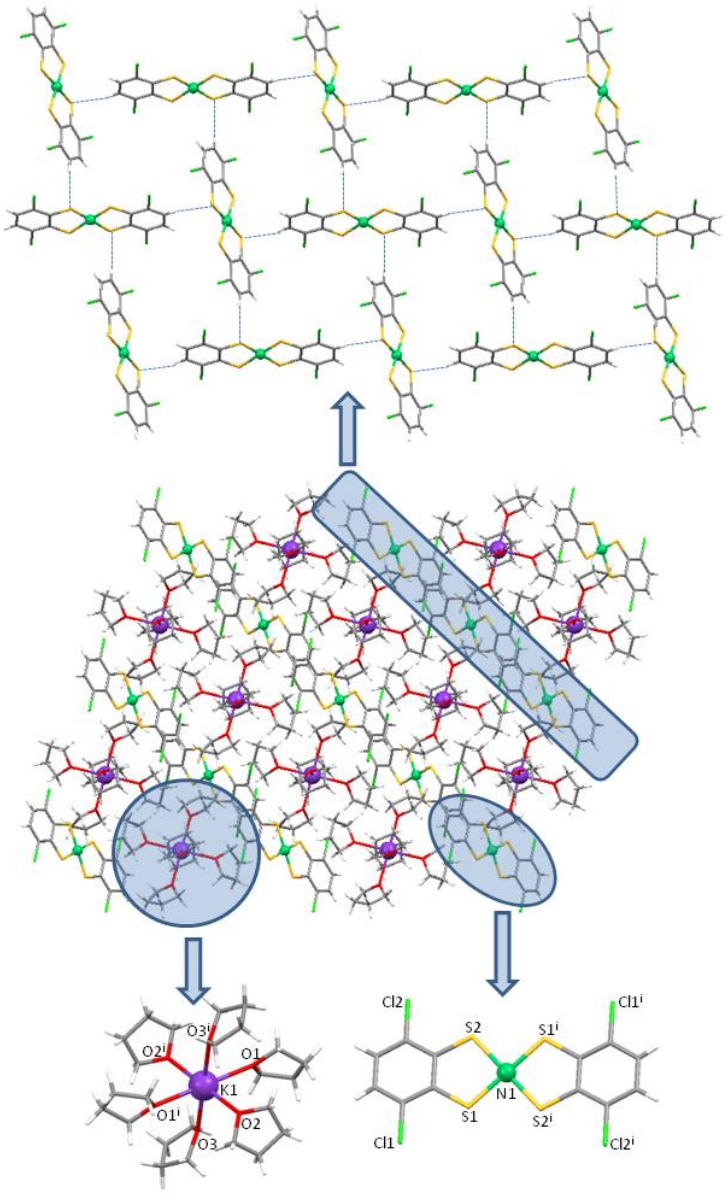

Figure 1. Monomeric $[K(thf)_6]^+$ and $[Ni(SC_6H_2Cl_2S)_2]^-$ entities found in compound **1**. Details on the supramolecular sheet of C-H···S assembled of $[Ni(SC_6H_2Cl_2S)_2]^-$ entities and overall cation-anion layered structure.

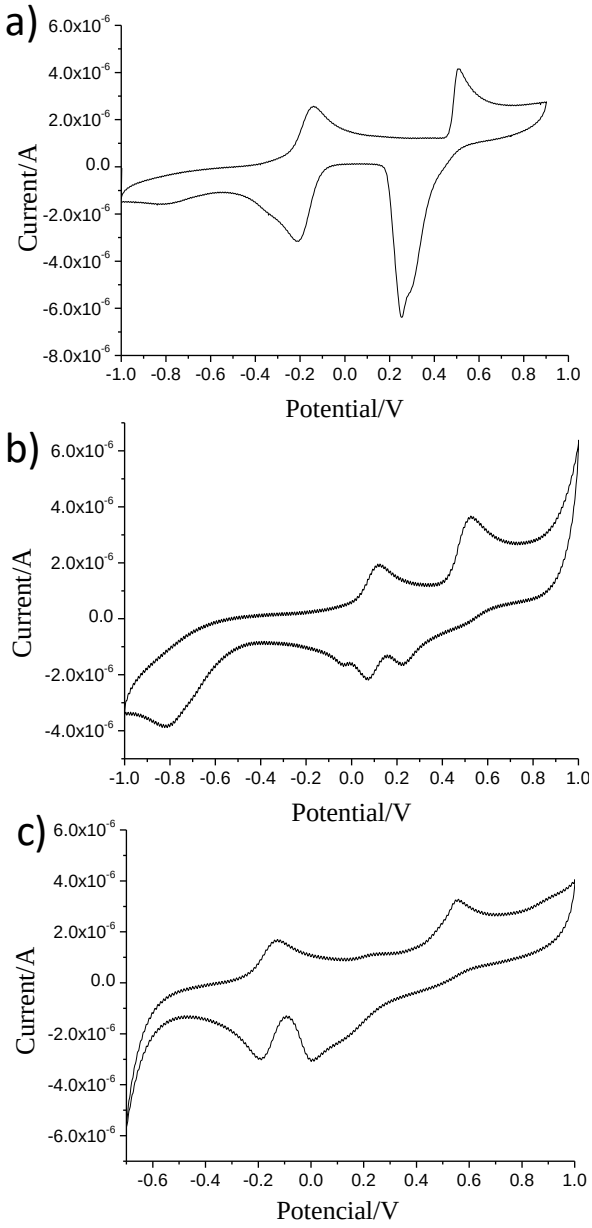

Figure 2. Cyclic voltamperograms of compounds $\{[K_2(\mu\text{-}H_2O)_2(\mu\text{-thf})(thf)_2][Ni(SC_6H_2Cl_2S)_2]\}_n$ (a), $\{[K_2(\mu\text{-}H_2O)_2(\mu\text{-thf})(thf)_2][Pd(SC_6H_2Cl_2S)_2]\}_n$ (b) and $\{[K_2(\mu\text{-}H_2O)_2(thf)_6][Pt(SC_6H_2Cl_2S)_2]\}_n$ (c), in MeOH containing 0.1 M of Bu_nPF_6 as electrolyte (scan rate 100 mVS^{-1}). All peaks potentials are given *vs*. Ag/AgCl (3MKCl) at 298 K.

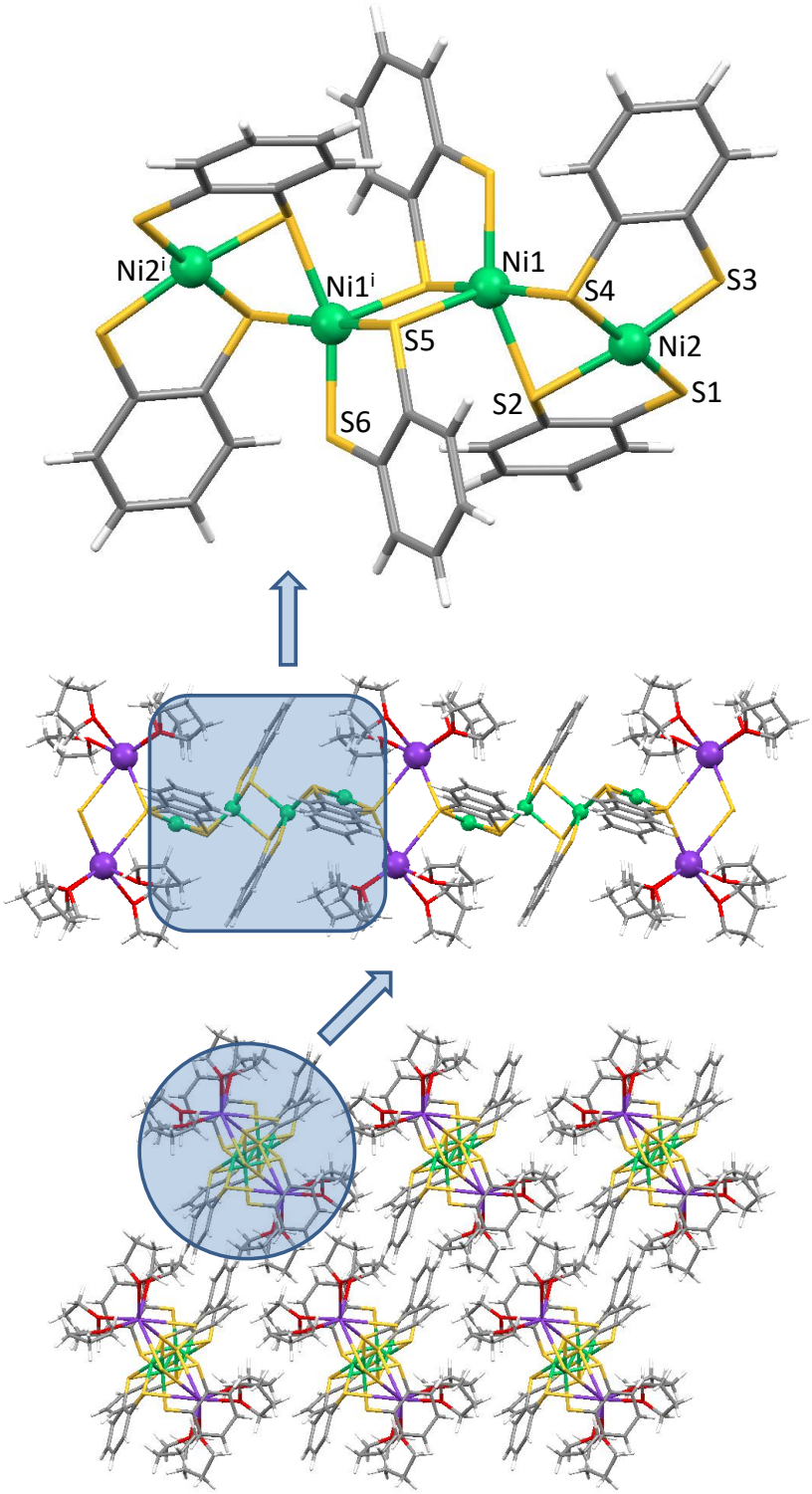

Figure 3. Tetrameric $[Ni_4(SC_6H_4S)_6]^{2-}$ entity, 1D coordination polymer and crystal packing viewed along its propagation direction in compound **3**.

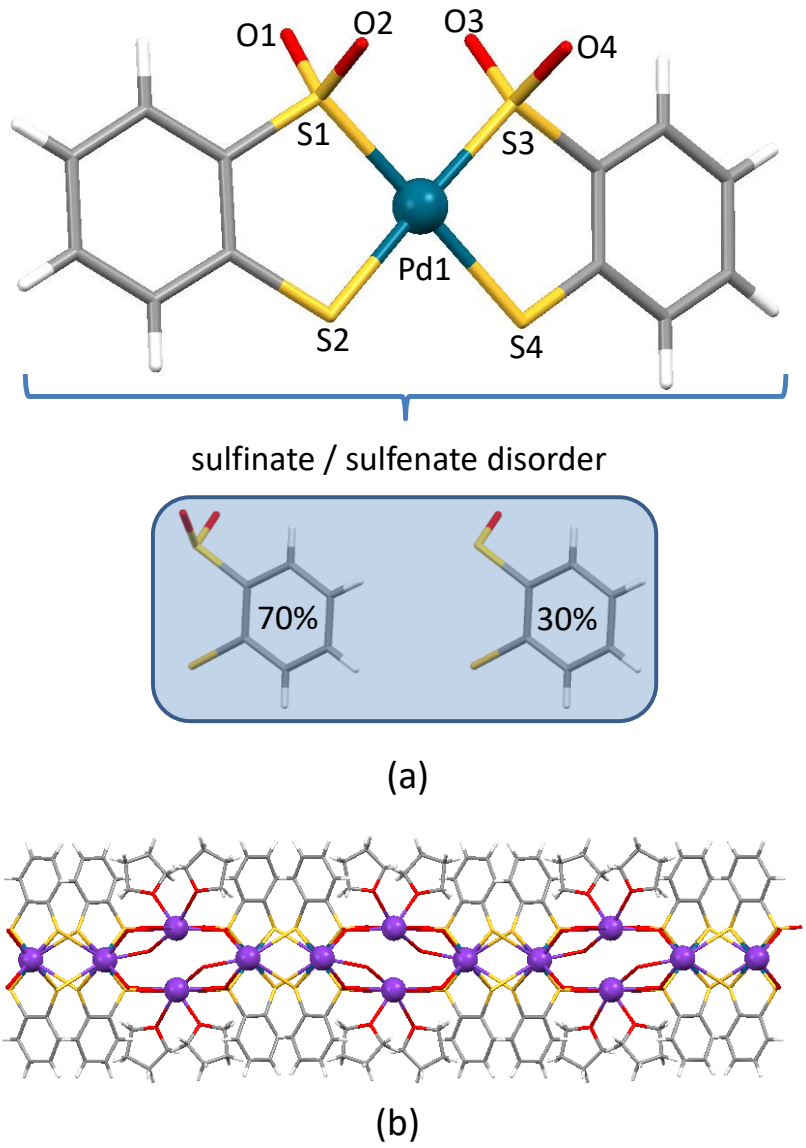

Figure 4. (a) $[Pd(O_2SC_6H_4S)_2]^{2-}$ entity emphasizing the 2-sulfanylbenzenesulfinate and 2-sulfanylbenzenesulfenate disorder in compound **4**. (b) Lateral view of the 2D coordination polymer.

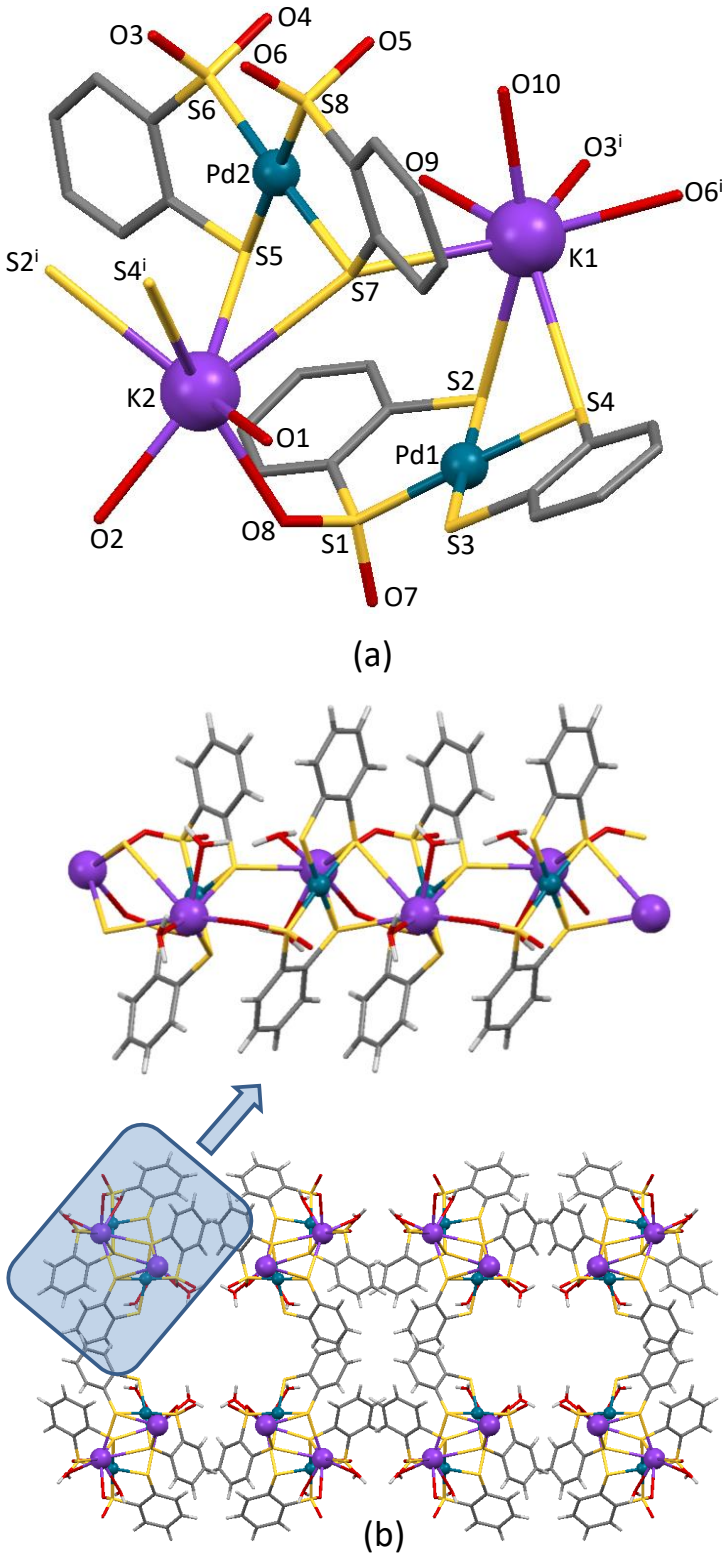

Figure 5. (a) Coordination environment and (b) crystal packing of the 1D coordination polymer in compound **5**.

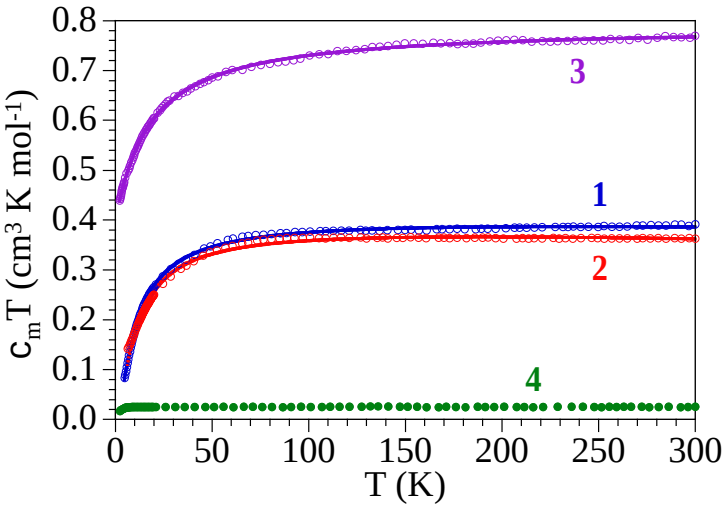

Figure 6. Thermal variation of $\chi_m T$ for compounds **1**-**4**. Solid lines are the best to the models (see text).

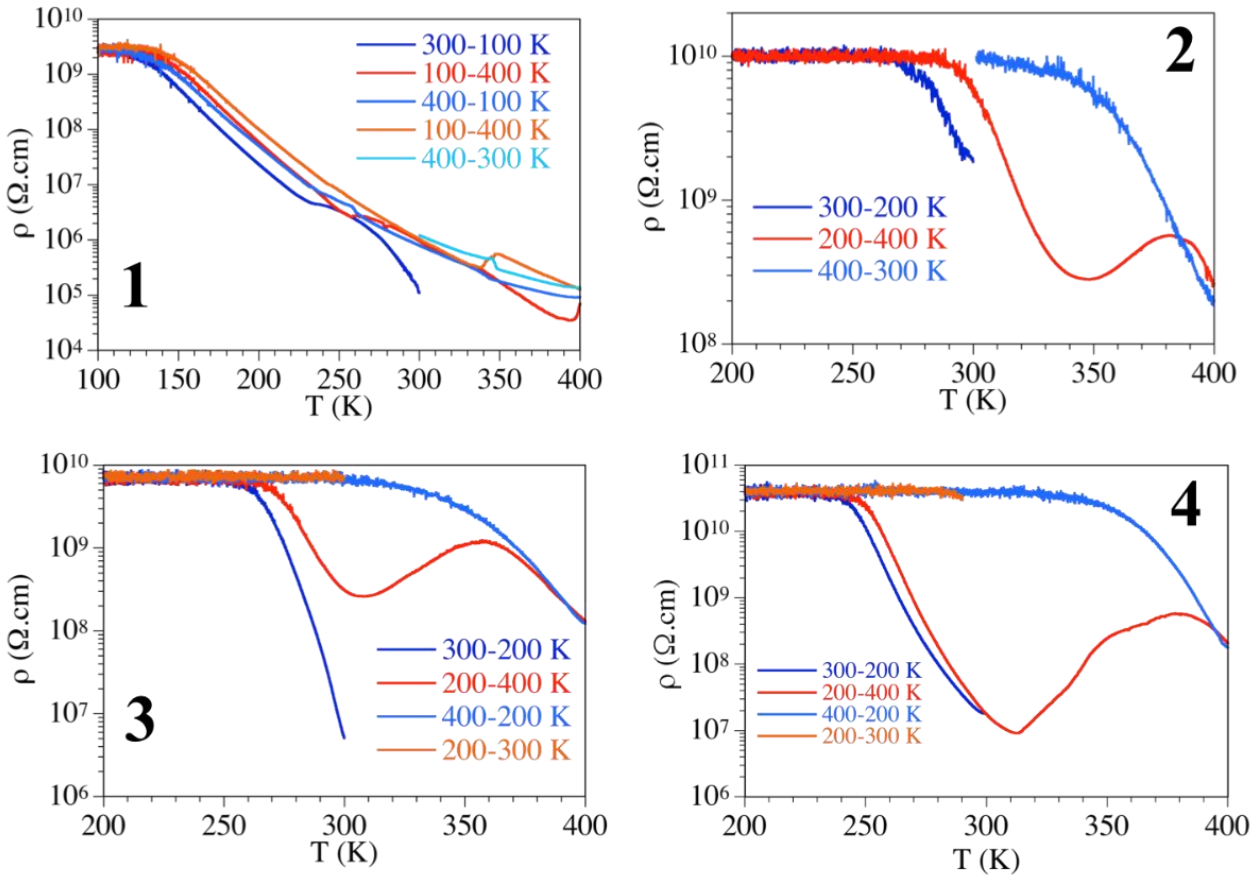

Figure 7. Thermal variation of the electrical resistivity of samples **1-4** during different cooling and heating scans.

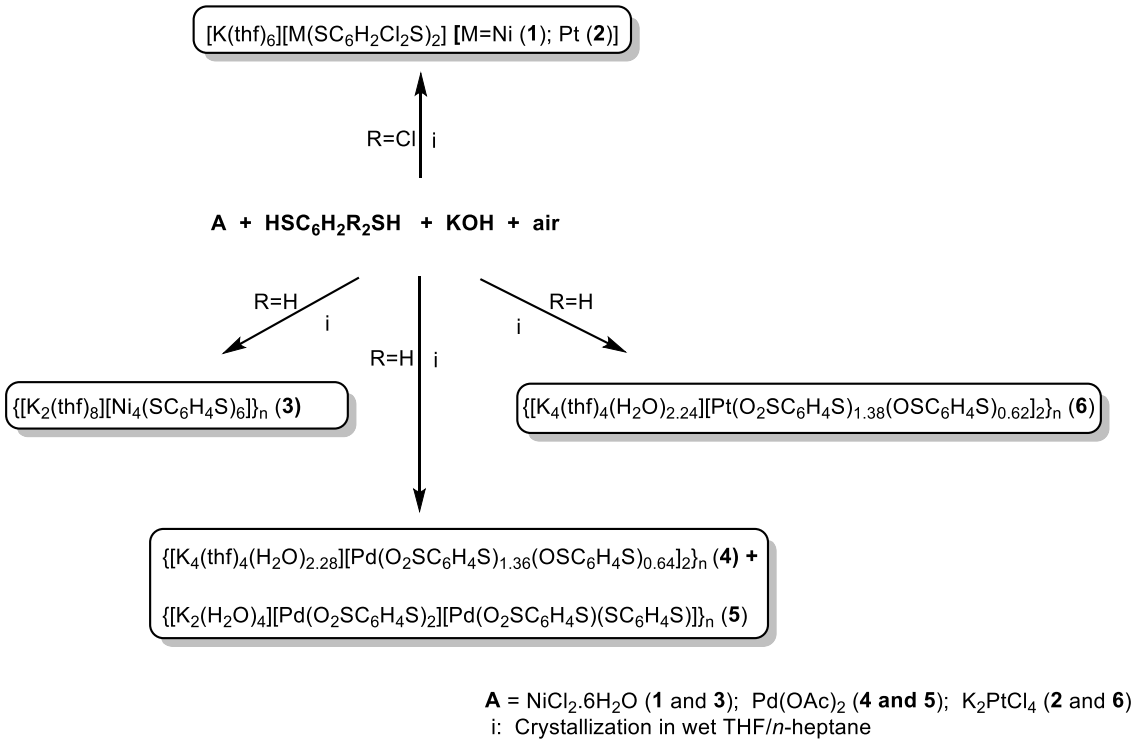

Scheme 1. Schematic representation of the syntheses of the compounds **1**-**6**.

Table 1. Crystallographic Data and Structure Refinement Details of Compounds **1-6**.

	1	**2**	**3**	**4**	**5**	**6**
formula	$C_{36}H_{52}Cl_4KNiO_6S_4$	$C_{36}H_{52}Cl_4KO_6PtS_4$	$C_{34}H_{44}KNi_2O_4S_6$	$C_{40}H_{52}K_4O_{13}Pd_2S_8$	$C_{24}H_{24}K_2O_{10}Pd_2S_8$	$C_{40}H_{52}K_4O_{13}Pt_2S_8$
M	948.62	1085	865.57	1366.49	1019.91	1543.87
T [K]	200(2)	200(2)	200(2)	200(2)	200(2)	200(2)
λ [Å]	0.71073	0.71073	0.71073	0.71073	0.71073	0.71073
crystal system	monoclinic	monoclinic	triclinic	monoclinic	orthorhombic	monoclinic
space group	$P2_1/n$	$P2_1/n$	P-1	$P2_1/c$	$P2aa$	$P2_1/c$
a [Å]	12.2033(8)	12.1700(13)	11.8592(9)	14.4496(4)	8.1121(9)	14.4013(4)
b [Å]	12.3432(9)	12.4010(10)	12.899(1)	23.6984(5)	21.0123(5)	23.7193(5)
c [Å]	15.8255(9)	15.8860(14)	14.4758(7)	7.8575(2)	23.590(5)	7.8356(2)
α [º]	90(-)	90(-)	105.182(5)	90(-)	90(-)	90(-)
β [º]	110.087(6)	109.710(6)	107.403(5)	99.4540(10)	90(-)	99.5350(10)
γ [º]	90(-)	90(-)	105.346(7)	90(-)	90(-)	90(-)
V [Å^3]	2238.8(3)	2257.1(4)	1892.6(3)	2654.12(11)	4021.0(10)	2639.58(11)
Z	2	2	2	2	4	2

ρ_{calcd} [g cm^{-3}]	1.407	1.596	1.519	1.710	1.685	1.942
μ [mm^{-1}]	0.990	3.662	1.472	1.363	1.561	5.984
F(000)	990	1090	902	1384	2024	1512
reflections collected	49461	38360	40514	43966	15241	44413
unique data	5138 (R_{int} = 0.0593)	46197 (R_{int} = 0.0477)	8670 (R_{int} = 0.111)	4863 (R_{int} = 0.0275)	8394 (R_{int} = 0.0549)	4856 (R_{int} = 0.0432)
reflections [I>2σ(I)]	3261	3238	5769	4034	5294	4212
goodness-of-fit on F^2 (S)[a]	1.028	1.001	1.139	1.079	1.002	1.058
R indices [I>2σ(I)][b]	*R*1 = 0.0512	*R*1 = 0.0379	*R*1 = 0.0643	*R1* = 0.0509	*R*1 = 0.0571	*R1* = 0.0379
	*wR*2 = 0.1345	*wR*2 = 0.0846	*wR*2 = 0.1181	*wR2* = 0.1322	*wR*2 = 0.1478	*wR2* = 0.0992
R indices (all data)[b]	*R*1 = 0.0930	*R*1 = 0.082	*R*1 = 0.1174	*R1* = 0.0638	*R*1 = 0.1023	*R1* = 0.0467
	*wR*2 = 0.1571	*wR*2 = 0.0981	*wR*2 = 0.1369	*wR2* = 0.1411	*wR*2 = 0.1653	*wR2* = 0.1046

[a] $S = [\sum w(F_0^2 - F_c^2)^2 / (N_{obs} - N_{param})]^{1/2}$. [b] $R1 = \sum||F_0|-|F_c|| / \sum|F_0|$. [c] $wR2 = [\sum w(F_0^2 - F_c^2)^2 / \sum wF_0^2]^{1/2}$; $w = 1/[\sigma^2(F_0^2) + (aP)^2 + bP]$ where $P = (\max(F_0^2,0) + 2Fc^2)/3$ with a = 0.0775 (**1**); 0.0377 (**2**); 0.0200 (**3**); 0.0643 (**4**); 0.0914 (**5**); 0.0621 (**6**); and b = 0.5778 (**1**); 0.9867 (**2**); 7.2855 (**3**); 11.5773 (**4**); 8.3468 (**6**).

Table 2. Electrical conductivity values and activation energies of compounds **1**-**4**.

Compound	M-R	σ_{300} (S/cm)	σ_{400} (S/cm)	E_a (meV)[a]	E_a (meV)[b]
1	Ni-Cl	4×10^{-5}	2×10^{-3}	200	200
2	Pt-Cl	4×10^{-8}	7×10^{-7}	400	800
3	Ni-H	5×10^{-7}	8×10^{-9}	770	960
4	Pd-H	2×10^{-8}	6×10^{-9}	1100	1400

[a]First cooling scan; [b]after heating at 400 K.

For Table of Contents Use Only

Title: Comparative Studies of Oxidation Processes on Group 10 Metals Dithiolene Derivatives in the Formation of Coordination Polymers

Authors: Oscar Castillo, Esther Delgado, Carlos J. Gómez-García, Diego Hernández, Elisa Hernández, Pilar Herrasti, Avelino Martín, and Félix Zamora

TOC Graphic:

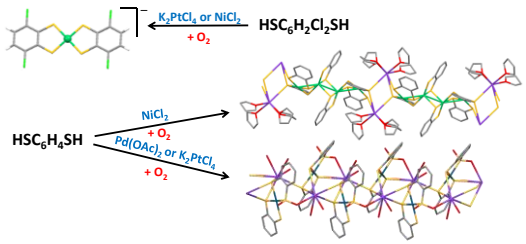

SYNOPSIS. Changes in dithiolene ligands coordinated to a group 10 metal center affect to the final product. Thus, oxidation of the dithiolene derivatives $\{[K_2(\mu\text{-}H_2O)_2(\mu\text{-}thf)(thf)_2][Ni(SC_6H_2Cl_2S)_2]\}_n$ and $\{[K_2(\mu\text{-}H_2O)_2(thf)_6][Pt(SC_6H_2Cl_2S)_2]\}_n$ give rise to the ion-pair compounds $[K(thf)_6][M(SC_6H_2Cl_2S)_2]$ [M = Ni or Pt]. Similar reactions carried out with $\{[K_2(\mu\text{-}H_2O)_x(thf)_y][M(SC_6H_4S)_2]\}_n$ (M= Ni, Pd, Pt) lead to the coordination polymers $\{[K_2(thf)_8][Ni_4(SC_6H_4S)_6]\}_n$, $\{[K_4(thf)_4(H_2O)_{2.28}][M(O_2SC_6H_4S)_{1.36}(OSC_6H_4S)_{0.64}]_2\}_n$ (M=Pd, Pt) and $\{[K_2(H_2O)_4][Pd(O_2SC_6H_4S)_2][Pd(O_2SC_6H_4S)(SC_6H_4S)]\}_n$.